# Lens Connexin Channels Have Differential Permeability to the Second Messenger cAMP

Virginijus Valiunas, Peter R. Brink, and Thomas W. White

The Renaissance Department of Physiology and Biophysics, Stony Brook University School of Medicine, Stony Brook, New York, United States

Correspondence: Thomas W. White, Renaissance Department of Physiology and Biophysics, Stony Brook University School of Medicine, T5-147, Basic Science Tower, Stony Brook, NY 11794-8661, USA; thomas.white@stonybrook.edu.

Submitted: April 9, 2019
Accepted: August 13, 2019

Citation: Valiunas V, Brink PR, White TW. Lens connexin channels have differential permeability to the second messenger cAMP. *Invest Ophthalmol Vis Sci*. 2019;60:3821–3829. https://doi.org/10.1167/iovs.19-27302

**Purpose.** Gap junction channels exhibit connexin specific biophysical properties, including the selective intercellular passage of larger solutes, such as second messengers. Here, we have examined the cyclic nucleotide permeability of the lens connexins, which could influence events like epithelial cell division and differentiation.

**Methods.** We compared the cAMP permeability through channels composed of Cx43, Cx46, or Cx50 using simultaneous measurements of junctional conductance and intercellular transfer. For cAMP detection, the recipient cells were transfected with a cAMP sensor gene, the cyclic nucleotide-modulated channel from sea urchin sperm (SpIH). cAMP was introduced via patch pipette into the cell of the pair that did not express SpIH. SpIH-derived currents were recorded from the other cell of a pair that expressed SpIH. cAMP permeability was also directly visualized in transfected cells using a chemically modified fluorescent form of the molecule.

**Results.** cAMP transfer was observed for homotypic Cx43 channels over a wide range of junctional conductance. Homotypic Cx46 channels also transferred cAMP, but permeability was reduced compared with Cx43. In contrast, homotypic Cx50 channels exhibited extremely low permeability to cAMP, when compared with either Cx43, or Cx46.

**Conclusions.** These data show that channels made from Cx43 and Cx46 result in the intercellular delivery of cAMP in sufficient quantity to activate cyclic nucleotide-modulated channels. The data also suggest that the greatly reduced cAMP permeability of Cx50 channels could play a role in the regulation of cell division in the lens.

Keywords: connexins, permeability, membrane channels, lens epithelium

Multicellular animals require communication between cells for the coordinated growth and development of tissues. This communication can derive from the binding of circulating growth factors to receptors that activate intracellular signal transduction cascades and generate second messengers, or be directly propagated between cells through the intercellular channels present in gap junctions. Both signal transduction pathways and gap junction channels are known to play important roles in the growth of the eye lens,[1–8] but no studies have yet addressed whether differences in second messenger permeability through connexin channels made of Cx43, Cx46, and Cx50 contribute to the intercellular communication necessary for normal lens growth.

Gap junctions were initially assumed to be nonselective[9,10]; however, experiments carefully examining the movement of ions and dyes between coupled cells have revealed connexin-dependent differences in permeation.[11–14] Innovative technical approaches have allowed this type of analysis to be extended to signaling molecules like $IP_3$ and cAMP.[15–19] Thus, different connexin channels are functionally distinct in terms of their conductance and permeability to small molecules.[15,16,20–22] Genetic studies in mice have documented that such functional differences between gap junction channel types are important, because the loss of one connexin cannot be compensated for by replacement with other connexins.[23–25]

Characterization of mouse models with single or double knock-outs and knock-ins of Cx43, Cx46, and Cx50 have found distinct roles for each lens connexin in vivo.[24,26–29] For example, a growth deficit in Cx50 knockout lenses is caused by a transient reduction in epithelial cell mitosis[7] that occurs on postnatal days 2 to 3 (P2–P3). Cx50 provides the majority of coupling between epithelial cells at this age, and functional replacement of Cx50 by Cx46 maintains the same magnitude of coupling, but does not restore normal cell division and lens growth.[24,30] Lens mitosis is stimulated by growth factors, which in turn activate intracellular signaling cascades.[31,32] Thus, it is possible that Cx50 and Cx46 have different permeability to the second messengers arising from growth factor–mediated signal transduction, resulting in a difference of recruitment of neighboring cells into mitosis on P2 to P3.

The lens presents an ideal system to explore differential permeability of gap junctions to second messengers, as it only expresses three connexins in two cell types.[1,33–35] Cx43 and Cx50 are present in epithelial cells, while Cx46 and Cx50 form the abundant gap junction channels between fibers.[34,36] There is also an extensive literature on the developmental consequences of genetic manipulation of lens connexins in mice,[33,34,37] that can be correlated with potential differences in second messenger permeation. Here, we have used patch clamp electrophysiologic and fluorescent imaging approaches to determine the permeation of cAMP through Cx43, Cx46, and Cx50 channels in vitro. We found that Cx43 and Cx46 were highly permeable to cAMP, whereas Cx50 channels exhibited extremely low permeability to this second messenger. Com-

bined with previously published work from Cx50-deficient mice,[7,24,26,30] these data suggest that the reduced cAMP permeability of Cx50 could play a role in the regulation of cell division in the postnatal lens.

## Materials and Methods

### Cell Culture

HeLa cells were plated on glass coverslips, grown to 50% confluence and transiently transfected with mouse Cx46 using Lipofectamine 2000 (Invitrogen, Carlsbad, CA, USA). Rat Cx43 and human Cx50 stably transfected HeLa cells[13,38] were also used.

### Electrophysiologic Measurements

A dual voltage-clamp method and whole-cell/perforated patch recording were used to control the membrane potential of paired cells and to measure currents.[13,39] Coverslips with adherent cells were transferred to a chamber on the stage of an inverted microscope equipped with fluorescence imaging. Cells were perfused at room temperature with bath solution containing (in mM) NaCl, 150; KCl, 10; $CaCl_2$, 2; HEPES, 5 (pH 7.4); glucose, 5; CsCl, 2; and $BaCl_2$, 2. Patch pipettes were filled with solution containing (in mM) $K^+$ aspartate$^-$, 120; NaCl, 10; MgATP, 3; HEPES, 5 (pH 7.2); EGTA, 10. For perforated patch experiments, the pipette solution contained 30 to 50 μM β-escin.[40] Pipettes were pulled from glass capillaries (Harvard Apparatus, Holliston, MA, USA) with a horizontal puller (DMZ-Universal, Zeitz-Instrumente, Martinsried, Germany). The resistance of the pipettes measured 2 to 5 MΩ.

### cAMP Flux Studies

cAMP transfer through connexin channels was investigated using cell pairs.[15,16] Recipient cells were transfected with the cyclic nucleotide-modulated channel from sea urchin (SpIH)[41,42] subcloned into pIRES2-EGFP (Takara Bio USA, Mountain View, CA, USA). Donor cells were transfected with red fluorescent protein (RFP; pIRES2-DsRed2; Takara Bio USA). SpIH and RFP-transfected cells were co-cultured. Green eGFP and red RFP signals were visualized under a fluorescent microscope and pairs consisting of one SpIH and one RFP-transfected cells were chosen for cAMP transfer measurements. cAMP was introduced via patch pipette into the cell of the pair that did not express SpIH, and SpIH-derived currents were recorded from the cell expressing SpIH. Five hundred micromolar of cAMP (Sigma-Aldrich, St. Louis, MO, USA) was dissolved in the pipette solution. To maintain a constant cytoplasmic concentration of cAMP during measurement of its permeation through connexin channels, the phospodiesterase inhibitor IBMX (200 μM; Sigma-Aldrich) was added to the bath solution to prevent degradation of exogenously delivered cAMP. An adenylate cyclase inhibitor 2′,5′-dideoxyadenosine (5 μM; Calbiochem, Burlington, MA, USA) was added to the pipette and bath solutions to prevent endogenous cAMP synthesis. Quantitative cAMP flux (molecules/channel/s) and unitary channel permeability (P) were calculated as described.[12,13,15,43]

### Fluorescent ε-cAMP Transfer

CAMP permeability was visualized in transfected cells using a fluorescent form of the molecule, 1, $N^6$-Ethenoadenosine-3′,5′-cyclic monophosphate (ε-cAMP; Biolog Life Science Institute, Bremen, Germany). ε-cAMP is an analogue of cyclic AMP in which the $N^1$ and the $N^6$ nitrogen atoms in the adenine nucleobase are connected by an etheno bridge to form a tricyclic ring system.[44,45] Five millimolar ε-cAMP was dissolved in the pipette solution. One cell in a pair, or cluster, was patched with a pipette containing ε-cAMP for up to 10 minutes to allow fluorescent cAMP passage from source cells to the adjacent cells. ε-cAMP was imaged at regular intervals using a digital CCD-camera (HRm Axiocam; Carl Zeiss, Thornwood, NY, USA). At the end of each cell pair experiment, the second cell was patched and the junctional current between the cells was measured.[16] The outline of each cell, and an area of background, were manually drawn in the image using ImageJ software (http://imagej.nih.gov/ij/; provided in the public domain by the National Institutes of Health, Bethesda, MD, USA).[46] Fluorescent intensities for recipient and source cells were corrected by subtracting the background intensity. Ratios of the corrected fluorescent intensities of the recipient to the source cell were calculated at the 5-minute time point.

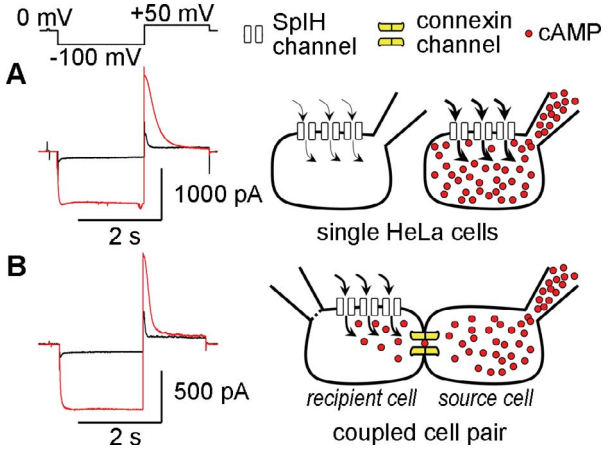


Figure 1. An electrophysiologic assay for intercellular transfer of cAMP through gap junction channels. (**A**) When single SpIH expressing cells were whole-cell patched without cAMP in the pipette (*cell on left*), SpIH currents were small (*black line*). When cAMP was present in the patch pipette (cell on *right*), SpIH currents were increased 4- to 5-fold (*red line*). (**B**) Cell pairs were co-cultured where one cell expressed the connexin to be tested and SpIH (recipient cell on *left*, cell 1). The other cell expressed only the connexin to be tested (source cell on *right*, cell 2). Five hundred micromolar cAMP was delivered via a whole-cell patch pipette into cell 2, and SpIH currents were recorded from cell 1 in the perforated patch mode, before (*black line*), and after (*red line*) opening the patch on cell 2.

### Statistical Analysis

Student's *t*-test or one-way ANOVA were used for two- or three-way comparisons of primary data, respectively (OriginLab, Northampton, MA, USA). Analysis of covariance (ANCOVA) was used to compare statistical differences between slopes fitted from linear regression (GraphPad Prism, San Diego, CA USA).

## Results

### Measurement of cAMP Permeability

We developed a method for the quantitative detection of cAMP transfer through connexin channels[15,16] (Fig. 1) using the SpIH[41] to detect cytoplasmic cAMP. In single cells, when no cAMP was delivered through the patch pipette, SpIH channels passed a low level of current (Fig. 1A, black line). When 50 μM cAMP was introduced into the cytoplasm through the patch

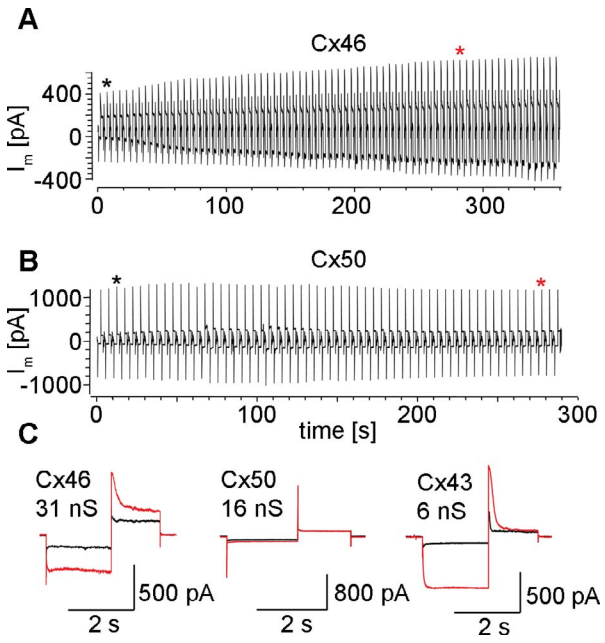


**Figure 2.** Cx46, but not Cx50, mediated intercellular transfer of cAMP. (**A**) Data from a Cx46 cell pair with a gap junctional conductance of 31 nS are shown. The SpIH current recorded from cell 1 over time, in response to voltage pulses of 0 to 100 mV, returning to a tail potential of +50 mV. At time 0, the patch in cell 2 was opened initiating cAMP delivery. The SpIH tail current over time increased approximately 4-fold. (**B**) Cx50 failed to mediate transfer of cAMP. The SpIH current remained constant in the recipient cell after 500μM cAMP was released in the source cell. This Cx50 cell pair had a gap junctional conductance of 16 nS. (**C**) Expanded SpIH currents from when the whole cell patch was first opened (*black asterisk/trace*), and 280 seconds later (*red asterisk/trace*). The Cx46 cell pair showed an approximately 4-fold increase in SpIH tail currents. For the Cx50 cell pair, the SpIH tail currents were of the same magnitude, indicating little, or no, intercellular cAMP transfer through Cx50 channels. Data from a Cx43 cell pair with a conductance of 6 nS are shown for comparison.

pipette, SpIH bound cAMP, producing an increased channel open probability and membrane current flow (Fig. 1A, red line). Detection of gap-junction–mediated movement of cAMP between cells was accomplished by co-culturing cell pairs where the recipient cell (cell 1) expressed the connexin to be tested and SpIH. The source cell (cell 2) expressed only the connexin to be tested. cAMP transfer was monitored by recording activity of the SpIH current in cell 1 before (Fig. 1B, black line), during, and after (Fig. 1B, red line), delivery of cAMP to cell 2. The gap junctional conductance between cells 1 and 2 was simultaneously measured. To maintain a constant cAMP concentration in the source cell, and prevent cAMP degradation in the recipient cell, phosphodiesterase and adenylate cyclase inhibitors were included in the culture medium and the pipette solution, respectively. The recipient cell was in the perforated patch mode to prevent cAMP from diffusing into the recipient cell pipette.

## Cx46 Channels Have Greater cAMP Permeability Than Cx50

Data obtained using the cAMP permeation assay in cell pairs expressing either Cx46 or Cx50 gap junction channels are shown in Figure 2. The source cell pipette contained 500 μM cAMP, and was opened in whole-cell mode at the time indicated by a black asterisk. In a Cx46 expressing cell pair with a junctional conductance of 31 nS, the magnitude of the SpIH current in the recipient cell increased following introduction of cAMP into the source cell (Fig. 2A), indicating the cell-to-cell passage of cAMP through Cx46 channels. In a Cx50 cell pair with a gap junctional conductance of 16 nS, the magnitude of the SpIH current did not change at all during the 5-minute period following introduction of cAMP into the donor cell (Fig. 2B), suggesting little, or no intercellular passage of cAMP through Cx50 channels. Expanded records of the SpIH current at the time when the whole-cell patch was first opened (Fig. 2C, black line), and 280 seconds later (red line) illustrated the different responses of the lens connexins. The cells transfected with Cx46 gap junction channels had an approximately 4-fold increase in the magnitude of the SpIH current. This showed that cAMP was being delivered from the source cell and could permeate through Cx46 channels. In the Cx50 expressing cell pair, there was no increase in the magnitude of the SpIH current. This suggested that very little cAMP was being delivered from the source cell, and that cAMP diffusion through Cx50 gap junction channels was negligible. For comparison, an expanded record from a cell pair with Cx43 channels showed that cAMP diffusion increased the magnitude of the SpIH current approximately 5-fold, as previously reported.[15] Thus, channels made of Cx43, Cx46, and Cx50 exhibited qualitatively different cAMP permeability.

## Comparison of Intercellular cAMP Transfer by Different Lens Connexins

Quantitation of differences in cAMP permeability between connexins was achieved by monitoring the time course of the increase in the SpIH dependent tail current relative to the junctional conductance between cells. The change in SpIH tail current was first plotted as a function of time for individual cell pairs expressing Cx46, Cx50, and Cx43 (Fig. 3A). For a Cx46 cell pair (open triangles), the tail current rose steadily to a new saturated value of approximately 200 pA within approximately 150 seconds following cAMP delivery to the source cell. In contrast, a Cx50 cell pair (open circles) showed a much slower rate of increase in SpIH tail current that did not reach saturation within 300 seconds. In a Cx43 cell pair (filled circles), the tail current rose rapidly to a new saturated value of approximately 1450 pA in approximately 20 seconds. For cell pairs expressing Cx43 and Cx46, primary data like these allowed calculation of the parameter $\Delta I/\Delta t$, which is the net change in the SpIH current normalized to its maximum value, divided by the net time required to attain the tail current increase as we have previously shown.[15] For the Cx43 cell pair shown in Figure 3A, $\Delta I/\Delta t$ was obtained by fitting the linear part of the current-time relationship (Fig. 3B, filled circles), and represents the SpIH current increase due to cAMP accumulation in the recipient cells, after permeation through connexin channels from the source cell. Data for the Cx46 cell pair (Fig. 3B, open triangles) required more time to reach saturation, resulting in a reduced slope compared with Cx43. In the 50% of Cx50 cell pairs where the SpIH current measurably increased, it never reached saturation during the finite period that cells could be recorded from, so $\Delta I/\Delta t$ had to be estimated from linear fits of the entire data sets that showed consistent SpIH current increase over time (Fig. 3C, open circles).

Data showing the increase in SpIH current following delivery of cAMP to the neighboring cell were collected from 7 to 10 individual cell pairs expressing either Cx43, Cx46, or Cx50. These aggregate data from all of the experiments were plotted in Figure 4. For Cx43 ($n = 9$) and Cx46 ($n = 7$), the SpIH tail current showed a 3.6 ± 0.6- and 2.6 ± 0.8-fold increase, respectively. In contrast, only half of the Cx50 cell

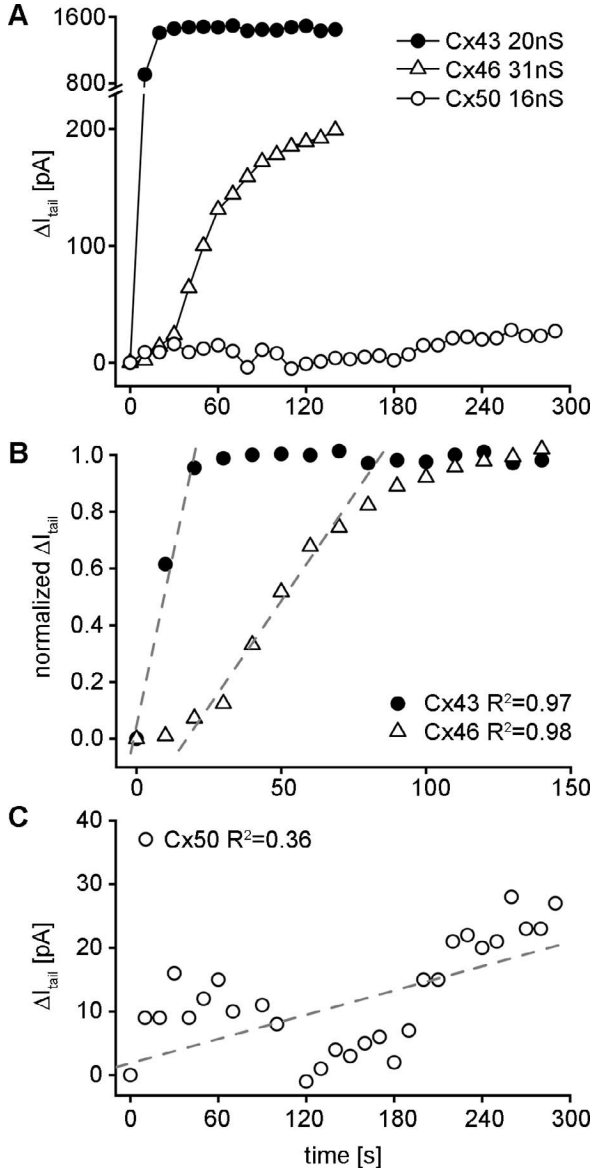


FIGURE 3. Quantitative comparison of intercellular cAMP transfer between the different lens connexins. (**A**) The change in the SpIH tail current was plotted versus time for individual cell pairs expressing Cx43 (*filled circles*), Cx46 (*open triangles*), or Cx50 (*open circles*). (**B**) A plot of the normalized tail current versus time recorded from the recipient cell after cAMP injection into the source cell for the Cx43 and Cx46 expressing cell pair. The SpIH activation time corresponds to the time when SpIH current reaches saturation in the recipient cell. The slopes of first order regressions over the linear part of the plot (*dashed lines*) were used to calculate the current activation rate ($\Delta I/\Delta t$). (**C**) Expanded view of the SpIH tail current data for the Cx50 cell pair shown in (**A**). In the Cx50 cell pairs where the SpIH current increased, it never reached saturation during the finite period that cells could be recorded from, so $\Delta I/\Delta t$ was estimated from fitting the current increase over the entire range of data available.

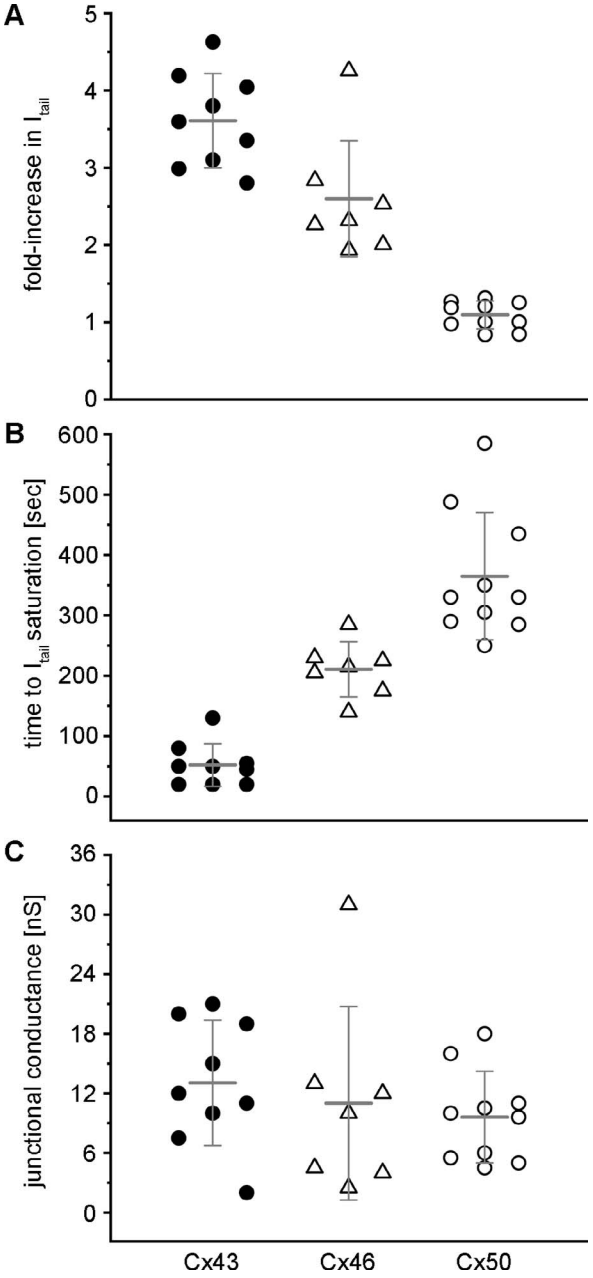


FIGURE 4. Summary quantification of SpIH current and gap junction conductance data. (**A**) The fold-increase in the SpIH tail current after cAMP delivery to the neighboring cell was plotted for individual cell pairs expressing Cx43 (*filled circles*, $n = 9$), Cx46 (*open triangles*, $n = 7$), or Cx50 (*open circles*, $n = 10$). Mean values of the data are plotted as *horizontal lines*, with standard deviations plotted as *vertical error bars*. (**B**) Plots of the time required for the SpIH tail current to reach saturation in Cx43 and Cx46 cell pairs. For Cx50, the time elapsed without the SpIH tail current reaching saturation was plotted. (**C**) Plots of the total gap junctional conductance measured between cell pairs expressing Cx43, Cx46, or Cx50.

pairs ($n = 10$) showed a SpIH current increase, resulting in a mean 1.1 ± 0.2-fold change (Fig. 4A, $P < 0.05$, one-way ANOVA). For Cx43, the mean time to SpIH tail current saturation was 52 ± 35 seconds, compared with 211 ± 45 seconds for Cx46. In all of the Cx50 expressing cell pairs, the SpIH tail current failed to reach saturation during the limited time frame that the cell pair could be stably recorded by dual whole-cell patch clamp (between 5 and 10 minutes). This limited us to plotting the elapsed time without achieving SpIH saturation for Cx50, which underestimates the actual saturation time, and had a mean value of 365 ± 105 seconds. Despite this underestimation, Cx50 showed a significantly slower response than either Cx43 or Cx46 (Fig. 4B, $P < 0.05$, one-way ANOVA). In contrast to the changes in SpIH tail current, the mean values of gap junctional conductance between the cell pairs for Cx43 (13 ± 6 nS), Cx46 (11 ± 10 nS), and Cx50

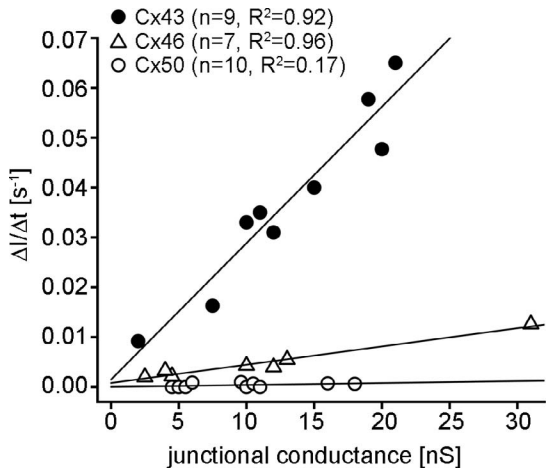


**Figure 5.** The SpIH current activation rate is dependent on the magnitude of gap junctional coupling between the cells. The SpIH tail current activation rate (*ΔI/Δt*) was plotted against gap junctional conductance for Cx43 (*filled circles*, $n = 9$), Cx46 (*open triangles*, $n = 7$), and Cx50 (*open circles*, $n = 10$). The *solid lines* correspond to first order regressions with the slopes given in the Table.

(10 ± 5 nS) were not significantly different from each other (Fig. 4C, $P > 0.05$, one-way ANOVA).

The time course of SpIH current saturation during cAMP transfer is dependent on the magnitude of gap junctional coupling between the cells, which can be directly measured, and the cAMP permeability of the connexin coupling them. To quantitate cAMP permeability, the ratio *ΔI/Δt* was plotted against junctional conductance for all data points generated from the three connexins (Fig. 5). The solid lines are linear fits with the significantly different ($P < 0.0001$, ANCOVA) slope values given in the Table. CAMP permeability was calculated using these slope values in combination with the known unitary conductance of the lens connexin channels, and our previously characterized behavior of SpIH in single cells when the concentration of cAMP was varied in the whole-cell patch pipette between 1 and 500 μM.[15] In single cells, intracellular delivery of cAMP increased SpIH currents in a dose-dependent manner. Fitting the linear part of the normalized tail current dose-response curve yielded a slope of 0.048/μM. This linear portion of the single cell dose–response curve corresponds to the linear part of the normalized SpIH tail current increase over time seen in cell pairs (Fig. 3B). *ΔI/Δt* allows estimation of the concentration of cAMP in the recipient cells by using the dose-response curve for the SpIH tail currents from single cells. For Cx46 channels, *ΔI/Δt* has a slope of 0.00037 $s^{-1}$/nS, and the cAMP flux can be calculated as follows: 0.00037 $s^{-1}$/nS ÷ ($0.048/10^{-6}$ M) = $7.71 \times 10^{-9}$ M/s/nS. The total number of cAMP molecules that transfer from the source cell to the recipient cell can also be calculated as the product of $(V_c)(\Delta C)(N_A)$, where $V_c$ is the cell volume, $\Delta C$ is the flux concentration, and $N_A$ is Avogadro's number. HeLa cells have an average volume of 1.8 pL,[47] so the total number of cAMP molecules that transfer to the recipient cell in 1s for a Cx46 junctional conductance of 1nS is (1.8 pL) ($7.71 \times 10^{-9}$ M/s/nS) ($6.02 \times 10^{23}$) = 8354 molecules/s/nS. Using the unitary conductance of Cx46 (146 pS),[48] the number of cAMP molecules passing per channel per second can be calculated as (8354 molecules/s/nS) (146 pS/channel ÷ 1nS) = 1220 molecules/channel/second. This cAMP permeability was 5-fold less than that calculated for Cx43 (6095 molecules/channel/second, Table).

For Cx50, cAMP permeability was estimated to be 35-fold less than that of Cx43, (176 molecules/channel/second, Table). However, it should be noted that in 5 of 10 experiments performed with Cx50 cell pairs there was no observed increase in SpIH (i.e., *ΔI/Δt* had a value of zero), which resulted in an $R^2$ value of 0.17 for the fit of the *ΔI/Δt* versus gap junctional conductance plot for Cx50 ($P = 0.23$). Despite the reduced level of certainty in our calculation of Cx50 permeability, these data clearly show that Cx43 and Cx46 channels have a much greater permeability to cAMP than Cx50.

## Optical Analysis of cAMP Passage Through Cx43 and Cx50 Channels

To confirm the significant difference in cAMP permeability between Cx43 and Cx50, we directly visualized cAMP permeability through lens connexin channels using a fluorescent form of the molecule (ε-cAMP). ε-cAMP has a long fluorescent lifetime, and retains the physiologic activity of native cAMP.[44,45] We initially tested the ability of ε-cAMP to permeate through Cx43 gap junction channels by attaching a pipette filled with the dye to a single cell within a small group of HeLa cells expressing Cx43 (Fig. 6A, $n = 6$). After opening the patch in whole-cell mode, dye transfer to half of the neighboring cells was detected within 5 minutes (Fig. 6B), and virtually all of the cells within 10 minutes (Fig. 6C), confirming that like native cAMP, ε-cAMP easily passed through Cx43 channels. When the experiment was repeated using Cx50 transfected HeLa cells (Fig. 6D, $n = 7$), very little transfer of ε-cAMP to neighboring cells was observed after either 5 (Fig. 6E) or 10 (Fig. 6F) minutes following the opening of the patch pipette.

To quantitatively compare the transfer of fluorescent cAMP through Cx43 and Cx50 channels, we performed simultaneous measurements of gap junction conductance and ε-cAMP fluorescent flux in isolated cell pairs.[13,16] Data are shown for a cell pair expressing Cx43 (Fig. 7A), where one patch pipette filled with ε-cAMP was attached to a single cell within the pair. The patch was opened in whole-cell mode, and ε-cAMP fluorescence was recorded for 5 minutes. At the end of fluorescent recording, the second cell was patched, and the magnitude of gap junctional conductance between the cells was determined to be 12 nS. Both cells in the Cx43 expressing pair had high levels of ε-cAMP fluorescence after 5 minutes (Fig. 7B). In contrast, a Cx50 cell pair with a gap junctional conductance of 16 nS (Fig. 7C) showed little passage of ε-cAMP

**Table.** cAMP Permeability of Cx43, Cx46, and Cx50 Channels

| Parameter | Cx43 | Cx46 | Cx50 |
|---|---|---|---|
| ΔI/Δt vs. $G_j$ slope ($s^{-1}$/nS) ± SE | $2.7 \pm 0.3 \times 10^{-3}$ | $3.7 \pm 0.3 \times 10^{-4}$ | $3.9 \pm 3 \times 10^{-5}$ |
| Unitary conductance (pS) | 55 | 146 | 200 |
| cAMP flux (molecules/channel/sec) | 6095 (5880*) | 1220 | 176 |
| Relative permeability ($cAMP/K^+$) | 0.18 | 0.014 | 0.0015 |
| Single channel permeability ($cm^3$/s) | $2.0 \times 10^{-14}$ | $4.1 \times 10^{-15}$ | $5.8 \times 10^{-16}$ |

* Previously calculated value for Cx43 from Kanaporis et al.[15]

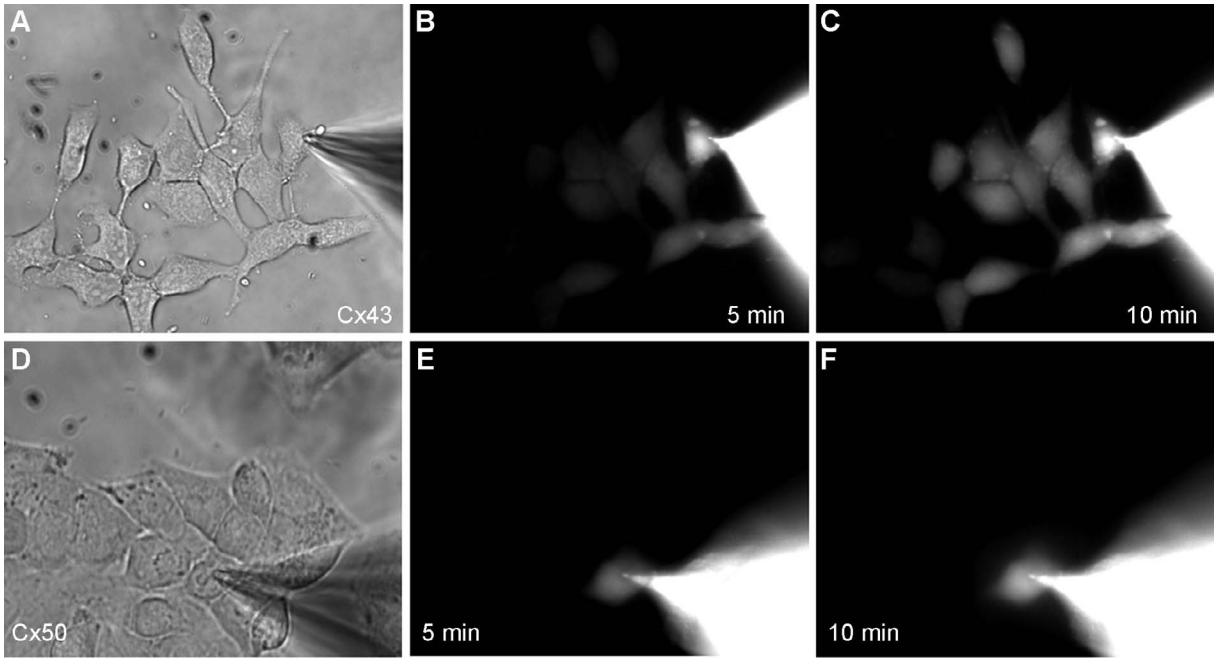


FIGURE 6. Visualization of cyclic nucleotide passage through Cx43 and Cx50 gap junction channels using fluorescent ε-cAMP. (**A**) A pipette filled with 5 mM ε-cAMP was attached to a single cell within a group of HeLa cells expressing Cx43. After opening the patch in whole-cell mode, (**B**) dye transfer was detected to half of the neighboring cells within 5 minutes, and (**C**) a majority of the cells within 10 minutes. (**D**) In Cx50 transfected HeLa cells, (**E**, **F**) negligible transfer of ε-cAMP to neighboring cells was observed at 5 or 10 minutes following the opening of the patch pipette.

to the second cell of the pair 5 minutes after the opening of the patch pipette (Fig. 7D). The mean (±SD) junctional conductance for cell pairs tested were 11 ± 1.4 and 17 ± 1.0 nS for Cx43 and Cx50, respectively (Fig. 7E, $n = 3$, $P > 0.05$, Student's *t*-test). The extent of ε-cAMP transfer was determined by calculating the ratio of fluorescent intensity in the recipient cell over that in the donor cell after 5 minutes. These ratios were 0.92 ± 0.18 for Cx43, and 0.09 ± 0.07 for Cx50 (Fig. 7F, $P < 0.05$, Student's *t*-test). Consistent with our results for native cAMP above, we found that ε-cAMP permeated through Cx43 channels much more readily than through Cx50 channels.

## DISCUSSION

We used two approaches to compare cAMP permeability through gap junction channels formed from different lens connexins, a quantitative electrophysiologic assay relying on activation of the SpIH channels,[15,16] and direct microscopic observation of the cell-to-cell passage of ε-cAMP, a fluorescent form of the molecule.[44,45] Using both approaches, Cx50 showed greatly reduced cAMP permeability compared with Cx43. Cx46 also had much greater cAMP permeability than Cx50, although not as high as that of Cx43. The calculated cAMP flux values for single gap junction channels were 6095,

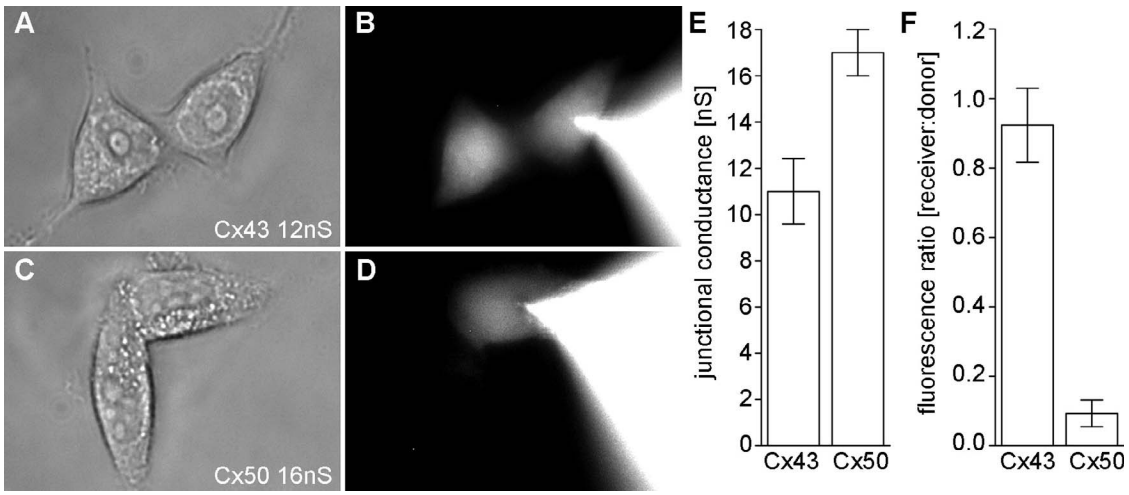


FIGURE 7. Quantitative comparison of ε-cAMP flux through Cx43 and Cx50 channels. Simultaneous measurements of gap junction conductance and ε-cAMP flux were made in cell pairs. (**A**) In a Cx43 expressing cell pair with conductance of 12 nS, (**B**) high levels of ε-cAMP fluorescence were recorded in the recipient cell 5 minutes after the patch pipette was opened in the donor cell. (**C**) In a cell pair expressing Cx50 with a conductance of 16 nS, (**D**) very little passage of ε-cAMP into the recipient cell was seen after 5 minutes. (**E**) The mean (±SD) conductance for all tested Cx43 and Cx50 cell pairs ($n = 3$). (**F**) The ratio of ε-cAMP fluorescent intensity in the recipient cell compared with the donor cell for Cx43 and Cx50.

1220, and 176 molecules/s for Cx43, Cx46, and Cx50, respectively (Table).

We performed our cAMP permeability experiments at room temperature (~25°C), and the conductance of connexin channels is moderately influenced by temperature with average $Q_{10}$ values of approximately 1.1 to 1.3.[49–53] However, it should be noted that the $Q_{10}$ value for an aqueous solution of KCl is 1.2 to 1.3,[54] which is the same magnitude as the values reported for connexin channels. This suggests that the modest temperature effects observed for connexin channel conductance are largely due to changes in solute mobility within the solvent. Connexin $Q_{10}$ values are not consistent with structural changes within the channel, but rather strongly suggest that the channel is dominated by solvent and not by interactions of solute with the channel wall. In the context of our work, the profound differences in cAMP permeability that we documented between Cx43, Cx46, and Cx50 channels are unlikely to vary significantly between 25°C and 37°C.

Knockout of Cx50 from the mouse lens resulted in decreased epithelial mitosis in the first postnatal week, and a significant reduction of lens growth.[7,26,55] In contrast, deletion of either Cx43 or Cx46 did not reduce mitosis or produce growth defects,[27,28] suggesting that a specific activity of Cx50 was required for normal postnatal epithelial mitosis and lens growth to occur. Cx50 provides most of the gap junctional coupling in the lens epithelia in the early postnatal period, and genetic replacement of Cx50 by Cx46 did not restore normal cell division, despite resulting in the same magnitude of junctional conductance between cells.[24,30] The intracellular concentration of cAMP oscillates during the cell cycle and significantly contributes to the regulation of the $G_0/G_1$ transition.[56,57] If differences in intrinsic cAMP permeability through connexin channels were important for normal epithelial cell division to proceed, then one could predict that neither Cx46 or Cx43 could replace the function of Cx50, as they both exhibit much greater permeability to cAMP.

Lens growth changes in the early postnatal period, where we observed a significant decrease in epithelial cell division in Cx50-deficient lenses.[7,30] During the preceding embryonic stage of lens growth, the diameter grows at a steady linear rate and the volume increases as a smooth exponential.[58,59] In contrast, early postnatal growth of the lens is oscillatory in a manner reproduced in organ culture by the pulsatile administration of growth factors, and that corresponds with the timing of the epithelial cell cycle.[60,61] Our data showed that Cx50 channels were much less permeable to cAMP than either Cx43 or Cx46. The elevation of cAMP levels directly affected proliferation in the lens epithelium,[62–64] and if Cx50 were the dominant connexin expressed when cells were actively dividing, its low intrinsic permeability would allow cells to autonomously regulate their cytoplasmic cAMP levels independently of their neighboring cells. In contrast, the high levels of cell-to-cell transfer of cAMP through Cx43 or Cx46 channels following the deletion, or genetic replacement of Cx50, could disrupt the epithelial cells ability to independently regulate their cytoplasmic cAMP due to flux between neighboring cells, and contribute to the altered cell proliferation seen in the mouse models.

Previous studies in mice have found a correlation between the functional activity of Cx50 and maximal postnatal proliferation in epithelial cells. On postnatal days 2 to 3, 20% or more of all lens epithelial cells were labeled following a 1-hour exposure to BrdU, and Cx50 provided 60% or more of the total magnitude of epithelial coupling. In older lenses, epithelial proliferation was reduced to 5% or less of total cells, and the contribution of Cx50 to gap junctional coupling was reduced to 25% or less by postnatal day 28, with the majority of coupling at this age provided by Cx43.[7,30] This correlation was further strengthened by the observations that postnatal epithelial cell proliferation was significantly reduced following the lens specific knockout of the p110α catalytic subunit of phosphoinositide 3-kinase, and that the magnitude of gap junctional conductance mediated by Cx50 channels was specifically upregulated by p110α.[8,65] Together, these studies have pinpointed a critical role for Cx50 channels in lens epithelial cell proliferation. Our current work has now identified profound differences in the permeability of the second messenger cAMP through lens connexin channels as one possible explanation for why Cx50 channels were required for the proper regulation of postnatal lens mitosis.

## Acknowledgments

Supported by National Institutes of Health (Bethesda, MD, USA) Grants EY013163 and EY026911 (TWW), and GM088181 (VV).

Disclosure: **V. Valiunas**, None; **P.R. Brink**, None; **T.W. White**, None

## References

1. Gerido DA, White TW. Connexin disorders of the ear, skin, and lens. *Biochim Biophys Acta*. 2004;1662:159–170.
2. Lovicu FJ. Cell signaling in lens development. *Semin Cell Dev Biol*. 2006;17:675.
3. McAvoy JW, Chamberlain CG, de Iongh RU, Hales AM, Lovicu FJ. Lens development. *Eye (Lond)*. 1999;13(Pt 3b):425–437.
4. Robinson ML. An essential role for FGF receptor signaling in lens development. *Semin Cell Dev Biol*. 2006;17:726–740.
5. Boswell BA, Lein PJ, Musil LS. Cross-talk between fibroblast growth factor and bone morphogenetic proteins regulates gap junction-mediated intercellular communication in lens cells. *Mol Biol Cell*. 2008;19:2631–2641.
6. Le AC, Musil LS. A novel role for FGF and extracellular signal-regulated kinase in gap junction-mediated intercellular communication in the lens. *J Cell Biol*. 2001;154:197–216.
7. Sellitto C, Li L, White TW. Connexin50 is essential for normal postnatal lens cell proliferation. *Invest Ophthalmol Vis Sci*. 2004;45:3196–3202.
8. Sellitto C, Li L, Vaghefi E, Donaldson PJ, Lin RZ, White TW. The phosphoinosotide 3-kinase catalytic subunit p110alpha is required for normal lens growth. *Invest Ophthalmol Vis Sci*. 2016;57:3145–3151.
9. Goodenough DA. Gap junction dynamics and intercellular communication. *Pharmacol Rev*. 1978;30:383–392.
10. Gilula NB, Reeves OR, Steinbach A. Metabolic coupling, ionic coupling and cell contacts. *Nature*. 1972;235:262–265.
11. Goldberg GS, Valiunas V, Brink PR. Selective permeability of gap junction channels. *Biochim Biophys Acta*. 2004;1662:96–101.
12. Kanaporis G, Brink PR, Valiunas V. Gap junction permeability: selectivity for anionic and cationic probes. *Am J Physiol Cell Physiol*. 2011;300:C600–C609.
13. Valiunas V, Beyer EC, Brink PR. Cardiac gap junction channels show quantitative differences in selectivity. *Circ Res*. 2002;91:104–111.
14. Veenstra RD, Wang HZ, Beblo DA, et al. Selectivity of connexin-specific gap junctions does not correlate with channel conductance. *Circ Res*. 1995;77:1156–1165.
15. Kanaporis G, Mese G, Valiuniene L, White TW, Brink PR, Valiunas V. Gap junction channels exhibit connexin-specific permeability to cyclic nucleotides. *J Gen Physiol*. 2008;131:293–305.
16. Mese G, Valiunas V, Brink PR, White TW. Connexin26 deafness associated mutations show altered permeability to large

cationic molecules. *Am J Physiol Cell Physiol*. 2008;295: C966–C974.

17. Ayad WA, Locke D, Koreen IV, Harris AL. Heteromeric, but not homomeric, connexin channels are selectively permeable to inositol phosphates. *J Biol Chem*. 2006;281:16727–16739.
18. Beltramello M, Piazza V, Bukauskas FF, Pozzan T, Mammano F. Impaired permeability to Ins(1,4,5)P3 in a mutant connexin underlies recessive hereditary deafness. *Nat Cell Biol*. 2005;7: 63–69.
19. Zhang Y, Tang W, Ahmad S, Sipp JA, Chen P, Lin X. Gap junction-mediated intercellular biochemical coupling in cochlear supporting cells is required for normal cochlear functions. *Proc Natl Acad Sci U S A*. 2005;102:15201–15206.
20. Bukauskas FF, Verselis VK. Gap junction channel gating. *Biochim Biophys Acta*. 2004;1662:42–60.
21. Harris AL. Connexin channel permeability to cytoplasmic molecules. *Prog Biophys Mol Biol*. 2007;94:120–143.
22. Harris AL. Emerging issues of connexin channels: biophysics fills the gap. *Q Rev Biophys*. 2001;34:325–472.
23. Plum A, Hallas G, Magin T, et al. Unique and shared functions of different connexins in mice. *Curr Biol*. 2000;10:1083–1091.
24. White TW. Unique and redundant connexin contributions to lens development. *Science*. 2002;295:319–320.
25. White TW. Nonredundant gap junction functions. *News Physiol Sci*. 2003;18:95–99.
26. White TW, Goodenough DA, Paul DL. Targeted ablation of connexin50 in mice results in microphthalmia and zonular pulverulent cataracts. *J Cell Biol*. 1998;143:815–825.
27. White TW, Sellitto C, Paul DL, Goodenough DA. Prenatal lens development in connexin43 and connexin50 double knockout mice. *Invest Ophthalmol Vis Sci*. 2001;42:2916–2923.
28. Gong X, Li E, Klier G, et al. Disruption of alpha3 connexin gene leads to proteolysis and cataractogenesis in mice. *Cell*. 1997;91:833–843.
29. Martinez-Wittinghan FJ, Sellitto C, Li L, et al. Dominant cataracts result from incongruous mixing of wild-type lens connexins. *J Cell Biol*. 2003;161:969–978.
30. White TW, Gao Y, Li L, Sellitto C, Srinivas M. Optimal lens epithelial cell proliferation is dependent on the connexin isoform providing gap junctional coupling. *Invest Ophthalmol Vis Sci*. 2007;48:5630–5637.
31. McAvoy JW, Chamberlain CG. Fibroblast growth factor (FGF) induces different responses in lens epithelial cells depending on its concentration. *Development*. 1989;107:221–228.
32. Zatechka SD Jr, Lou MF. Studies of the mitogen-activated protein kinases and phosphatidylinositol-3 kinase in the lens. 1. The mitogenic and stress responses. *Exp Eye Res*. 2002;74: 703–717.
33. Mathias RT, White TW, Gong X. Lens gap junctions in growth, differentiation, and homeostasis. *Physiol Rev*. 2010;90:179–206.
34. Berthoud VM, Minogue PJ, Osmolak P, Snabb JI, Beyer EC. Roles and regulation of lens epithelial cell connexins. *FEBS Lett*. 2014;588:1297–1303.
35. Kar R, Batra N, Riquelme MA, Jiang JX. Biological role of connexin intercellular channels and hemichannels. *Arch Biochem Biophys*. 2012;524:2–15.
36. White TW, Bruzzone R. Intercellular communication in the eye: clarifying the need for connexin diversity. *Brain Res Brain Res Rev*. 2000;32:130–137.
37. Jiang JX. Gap junctions or hemichannel-dependent and independent roles of connexins in cataractogenesis and lens development. *Curr Mol Med*. 2010;10:851–863.
38. Berthoud VM, Minogue PJ, Guo J, et al. Loss of function and impaired degradation of a cataract-associated mutant connexin50. *Eur J Cell Biol*. 2003;82:209–221.
39. Valiunas V, Gemel J, Brink PR, Beyer EC. Gap junction channels formed by coexpressed connexin40 and connexin43. *Am J Physiol Heart Circ Physiol*. 2001;281:H1675–H1689.
40. Fan JS, Palade P. Perforated patch recording with beta-escin. *Pflugers Arch*. 1998;436:1021–1023.
41. Gauss R, Seifert R, Kaupp UB. Molecular identification of a hyperpolarization-activated channel in sea urchin sperm. *Nature*. 1998;393:583–587.
42. Shin KS, Rothberg BS, Yellen G. Blocker state dependence and trapping in hyperpolarization-activated cation channels: evidence for an intracellular activation gate. *J Gen Physiol*. 2001;117:91–101.
43. Hernandez VH, Bortolozzi M, Pertegato V, et al. Unitary permeability of gap junction channels to second messengers measured by FRET microscopy. *Nat Methods*. 2007;4:353–358.
44. Secrist JA III, Barrio JR, Leonard NJ, Villar-Palasi C, Gilman AG. Fluorescent modification of adenosine 3′,5′-monophosphate: spectroscopic properties and activity in enzyme systems. *Science*. 1972;177:279–280.
45. Secrist JA III, Barrio JR, Leonard NJ, Weber G. Fluorescent modification of adenosine-containing coenzymes. Biological activities and spectroscopic properties. *Biochemistry*. 1972; 11:3499–3506.
46. Schneider CA, Rasband WS, Eliceiri KW. NIH Image to ImageJ: 25 years of image analysis. *Nat Methods*. 2012;9:671–675.
47. Rackauskas M, Verselis VK, Bukauskas FF. Permeability of homotypic and heterotypic gap junction channels formed of cardiac connexins mCx30.2, Cx40, Cx43, and Cx45. *Am J Physiol Heart Circ Physiol*. 2007;293:H1729–H1736.
48. Hopperstad MG, Srinivas M, Spray DC. Properties of gap junction channels formed by Cx46 alone and in combination with Cx50. *Biophys J*. 2000;79:1954–1966.
49. Valiunas V, Manthey D, Vogel R, Willecke K, Weingart R. Biophysical properties of mouse connexin30 gap junction channels studied in transfected human HeLa cells. *J Physiol*. 1999;519(Pt 3):631–644.
50. Valiunas V, Weingart R. Electrical properties of gap junction hemichannels identified in transfected HeLa cells. *Pflugers Arch*. 2000;440:366–379.
51. Sakai R, Elfgang C, Vogel R, Willecke K, Weingart R. The electrical behaviour of rat connexin46 gap junction channels expressed in transfected HeLa cells. *Pflugers Arch*. 2003;446: 714–727.
52. Bukauskas FF, Elfgang C, Willecke K, Weingart R. Biophysical properties of gap junction channels formed by mouse connexin40 in induced pairs of transfected human HeLa cells. *Biophys J*. 1995;68:2289–2298.
53. Bukauskas FF, Weingart R. Temperature dependence of gap junction properties in neonatal rat heart cells. *Pflugers Arch*. 1993;423:133–139.
54. Robinson RA, Stokes RH. *Electrolyte Solutions*. Mineola, NY: Dover Publications; 2002.
55. Sikic H, Shi Y, Lubura S, Bassnett S. A stochastic model of eye lens growth. *J Theor Biol*. 2015;376:15–31.
56. Abell CW, Monahan TM. The role of adenosine 3′,5′-cyclic monophosphate in the regulation of mammalian cell division. *J Cell Biol*. 1973;59:549–558.
57. Friedman DL. Role of cyclic nucleotides in cell growth and differentiation. *Physiol Rev*. 1976;56:652–708.
58. Foster FS, Zhang M, Duckett AS, Cucevic V, Pavlin CJ. In vivo imaging of embryonic development in the mouse eye by ultrasound biomicroscopy. *Invest Ophthalmol Vis Sci*. 2003; 44:2361–2366.
59. Mu J, Slevin JC, Qu D, McCormick S, Adamson SL. In vivo quantification of embryonic and placental growth during

gestation in mice using micro-ultrasound. *Reprod Biol Endocrinol*. 2008;6:34.

60. Brewitt B, Clark JI. Growth and transparency in the lens, an epithelial tissue, stimulated by pulses of PDGF. *Science*. 1988; 242:777–779.
61. Brewitt B, Teller DC, Clark JI. Periods of oscillatory growth in developing ocular lens correspond with cell cycle times. *J Cell Physiol*. 1992;150:586–592.
62. Von Sallmann L, Grimes P. Effects of isoproterenol and cyclic AMP derivatives on cell division in cultured rat lenses. *Invest Ophthalmol*. 1974;13:210–218.
63. Grimes P, Von Sallmann L. Possible cyclic adenosine monophosphate mediation in isoproterenol-induced suppression of cell division in rat lens epithelium. *Invest Ophthalmol*. 1972;11:231–235.
64. Ireland ME, Tran K, Mrock L. Beta-adrenergic mechanisms affect cell division and differentiation in cultured chick lens epithelial cells. *Exp Eye Res*. 1993;57:325–333.
65. Martinez JM, Wang HZ, Lin RZ, Brink PR, White TW. Differential regulation of Connexin50 and Connexin46 by PI3K signaling. *FEBS Lett*. 2015;589:1340–1345.

Investigative Ophthalmology & Visual Science